International Forum on Aeroelasticity and Structural Dynamics
IFASD 2024
17-21 June 2024 The Hague, The Netherlands

# FLIGHT-DYNAMICS AND AEROELASTIC COUPLING IN FLEXIBLE MANEUVERING AIRCRAFT

**Dor Naftaly*** **and Daniella E. Raveh**[†1]

**Keywords:** Flight-dynamics and aeroelastic coupling; Maneuvering aircraft; Nonlinear dynamics; Large deformations; Stability analysis

**Abstract:** The paper presents a study of the coupled flight-dynamics and aeroelasticity of flexible vehicles, with focus on the impact of hard maneuvers on the aircraft's stability. The paper presents an original derivation of the nonlinear coupled equations of motion, their subsequent linearization, and a modal representation of the linearized equations of motion. The inertial coupling terms are examined to elucidate their magnitude and influence on the system's stability. A stability analysis of the coupled flight-dynamics-aeroelastic system for a flying wing UAV configuration is presented, highlighting the impact of maneuvering on the system's flutter onset speed and characteristics.

## 1 INTRODUCTION

In highly flexible aircraft, or in aircraft that undergo hard maneuvers, the coupling between the vehicle's flight dynamics and the aeroelastic response becomes significant and may impact the vehicle's performance. Several frameworks (e.g., [1, 2]) have been developed for performance analysis of very flexible wings, aimed at evaluation of their aerodynamic and aeroelastic characteristics, and the coupling of flight dynamics and aeroelastic responses. These frameworks vary in the aerodynamic and structural models used and the approach to their coupling. For static analyses, the structural model adopted should accurately represent the large deformations of the very flexible structure. The aerodynamic model should account for changes in the aerodynamic loading due to geometrical variations, including local elastic angles of attack, variation in force orientation, and wake roll-up effects. The dynamic analysis must couple flight dynamics with the elastic response since, for very flexible configurations, the natural structural frequencies are comparable to those in the flight dynamics, which might lead to Body Freedom Flutter (BFF) instability. [3]

Time-domain simulations of free aircraft rely on the integration of flight dynamics, structural dynamics, and aerodynamics. These disciplines are closely coupled, especially when considering nonlinearities. The main couplings involved are the aerodynamic coupling and the inertial coupling, and their significance depends on the vehicle's flexibility (i.e., typical linear flexibility or highly flexible configuration) and the maneuver's intensity (i.e., light or hard maneuver). Under the conditions of small deformations and light maneuvering, the inertial coupling is negligible compared to the aerodynamic coupling, as demonstrated by Francesco *et al.* [4]. Indeed, the common approach is to solve the flight dynamics and aeroelastic problems independently, taking into account only the mutual aerodynamic influences. However, for very flexible configurations and in hard maneuvers, the inertial coupling is non-negligible, calling for a coupled flight-mechanics aeroelastic solution.

*Ph.D. Student, Faculty of Aerospace Engineering, dor.naf01@gmail.com
†Professor, Faculty of Aerospace Engineering, daniella@technion.ac.il

The aerodynamic coupling includes the impact of rigid-body motion on the elastic response, which mainly involves the loads that cause the elastic response, and the influence of the elastic motion on the rigid-body aerodynamic coefficients and stability, as shown by Baldelli *et al.* [5]. In flying wing configurations, the coupling of the rigid body and elastic motions might lead to Body Freedom Flutter (BFF) instability when the flight mechanics frequencies are close to the aeroelastic frequencies. [3, 6]

The inertial coupling involves rigid-elastic acceleration coupling terms, which we refer to herein as *strong coupling*, and *weak coupling* terms that do not involve accelerations. [1] Most of the studies on flight dynamics of flexible aircraft focused on small deformations.Some studies also neglected the variation in the moment of inertia due to elastic deformation. [4,5,7–9] Francesco *et al.* [4] derived the EOM using linear elasticity while neglecting the body axes rotation terms in the derivation of the elastic EOM, which is valid only for light maneuvers.

The aerodynamic models used in flight dynamics of flexible configurations studies vary. Schmidt *et al.* [10] based his aerodynamic model on aerodynamic derivative coefficients due to rigid and elastic motions. Baldelli *et al.* [5] used a state-space unsteady aerodynamic model computed via rational function approximation (RFA) of frequency-domain aerodynamics computed by a linear panel model in the ZAERO commercial software [11]. Those models are valid only for light maneuvers, small induced angles, and small elastic deformations. Palacios *et al.* [12] studied the flight dynamics of highly flexible UAVs using a nonlinear beam structural model and various aerodynamic models, including UVLM. They demonstrated the impact of high deformation on the integral lift coefficient characteristics.

The current study investigates the nonlinear flight dynamics of hard maneuvering flexible aircraft. The paper introduces a unique derivation of the nonlinear coupled flight dynamics and aeroelastic EOM that is applicable even for large deformations. The study focuses on the inertial coupling presenting and discussing the significance of each inertial coupling term. For stability analysis, the nonlinear flight dynamics and aeroelastic EOM are linearized about a nominal steady condition and are presented in modal coordinates. A test case presents stability analysis of the coupled flight-dynamics-aeroelastic system for a flying wing configuration, demonstrating the impact of maneuvering on the system's flutter onset speed and characteristics.

## 2 MATHEMATICAL MODEL

### 2.1 Inertial Model

The location vector of all points on the deformed body can be written as:[2]:

$$\overline{r}_{bi} = \underline{\widetilde{I}} \cdot \vec{r}_0 + \overline{r}_b \tag{1}$$

where $\overline{r}_{bi}$ is the position of the deformed-structure grids in the Inertial frame, $\overline{r}_b$ is the position of the deformed-structure grids in a Local frame, and $\vec{r}_0$ is the position of the Local frame's origin in the Inertial frame. The local frame can be defined in various ways, as reviewed in Appendix A. $\underline{\widetilde{I}} \in \mathbb{R}^{3N\times 3}$ (where N is the number of nodes in the structural model) is the

[1] We refer to the acceleration coupling as *strong coupling* since it requires the concurrent solution of the rigid-body translation, rotation, and elastic EOM sets.

[2] Note that all physical vectors are marked with $\vec{()}$, and all algebraic vectors are marked with $\overline{()}$, all unit vectors are marked with $\hat{()}$, all matrices are marked with $\underline{()}$, all duplicated assembly matrices are marked with $\underline{\tilde{()}}$

duplication of the identity matrix $\underline{I} \in \mathbb{R}^{3\times3}$, defined as:

$$\widetilde{\underline{I}} = \begin{bmatrix} \underline{I} \\ \underline{I} \\ \vdots \\ \underline{I} \end{bmatrix} \tag{2}$$

$\overline{r}_b$ can be written as the sum of the non-deformed grids' position, $\overline{r}_{b0}$, and their elastic deformation, $\overline{u}_e$, such that:

$$\overline{r}_b = \overline{r}_{b0} + \overline{u}_e \tag{3}$$

Figure 1 shows an example of a single grid's position, where $X_I, Y_I, Z_I$ and $X_b, Y_b, Z_b$ are the coordinates of the Inertial and Local frames, respectively.

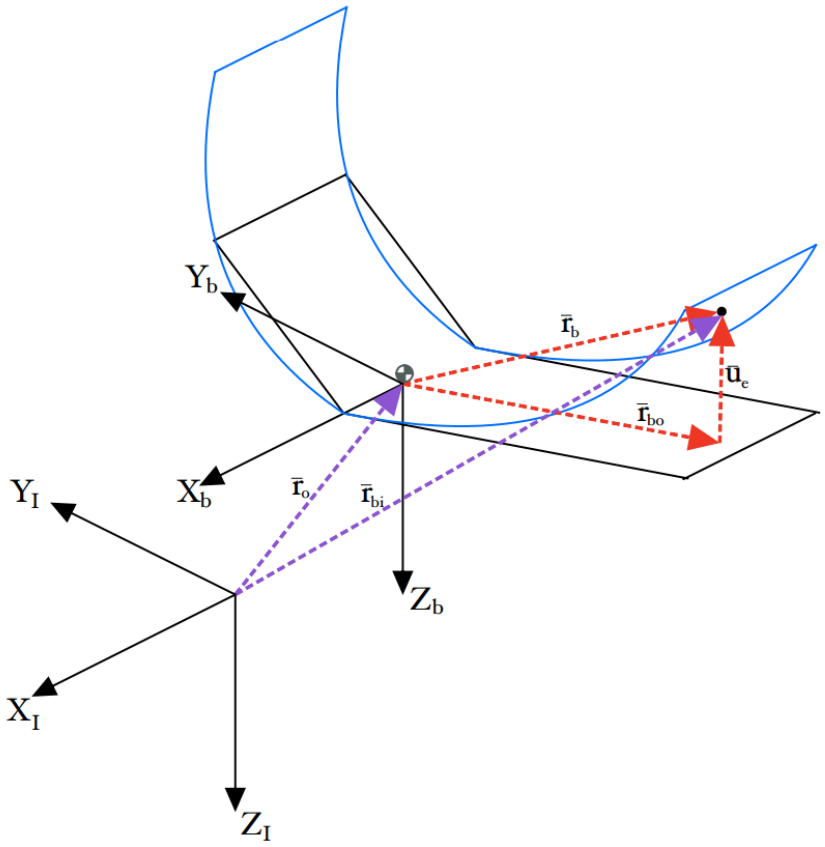


Figure 1: Visualization of the various position vectors

The mass and the moment of inertia matrices of the continuous structure about the Local frame's origin are defined as:

$$m = \iiint_V \rho \, dV \qquad \underline{I}_M = \iiint_V \rho(\vec{r} \cdot \vec{r} \cdot \underline{I} - \vec{r} \cdot \vec{r}^T) \, dV = \iiint_V \rho \underline{R}^T \cdot \underline{R} \, dV \tag{4}$$

where $\vec{r} = \begin{bmatrix} x & y & z \end{bmatrix}^T$ is a position vector (integration parameters with respect to the Local

frame). $\underline{R}$ is the skew-symmetric representation[3] of $\vec{r}$, defined as:

$$\underline{R} = \begin{bmatrix} 0 & -z & y \\ z & 0 & -x \\ -y & x & 0 \end{bmatrix} \tag{5}$$

By discretizing the structural representation, we can form the discretized mass matrix $\underline{M} \in \mathbb{R}^{3N\times 3N}$, where $M_{i,j}$ is defined as the force in the $i^{th}$ DOF due to a unit inertial acceleration in the $j^{th}$ DOF (both expressed in the Local frame).

Here, we assume that the structure's mass is discretized using a lumped-mass approach [13], in which each point mass, at each node, has three independent translational DOFs. The resulting mass matrix is diagonal since acceleration in one DOF only generates an inertial force in the same DOF. This holds true even for large deformations; thus, the mass matrix of the deformed structure is also diagonal and identical to the mass matrix of the undeformed structure. The mass matrix, therefore, remains constant over time for any elastic deformation, i.e.,

$$\dot{\underline{M}} = 0 \tag{6}$$

The mass matrix might be non-diagonal when the nodes have rotational DOFs, in consistent-mass discretization [13], or when the lumped-mass matrix is condensed. We note that, unlike the lumped-mass matrix, the stiffness matrix does change with elastic deformation, implying that it needs to be recalculated for the deformed geometry.

The integral mass and moment of inertia matrices (about the Local frame's origin) can be expressed in terms of the discretized mass matrix as:

$$m\underline{I} = \widetilde{\underline{I}}^T \cdot \underline{M} \cdot \widetilde{\underline{I}} \qquad \underline{I}_M = \underline{R}_b^T \cdot \underline{M} \cdot \underline{R}_b \tag{7}$$

where $\underline{R}_b \in \mathbb{R}^{3N\times 3}$ is

$$\underline{R}_b = \begin{bmatrix} \underline{R}_{b_1} \\ \underline{R}_{b_2} \\ \vdots \\ \underline{R}_{b_N} \end{bmatrix} \tag{8}$$

and where $\underline{R}_{b_i}$ is the skew symmetric representation (eq. 5) of $\vec{r}_{b_i}$, the position of deformed node $i$.

The CG location with respect to the origin of the Inertial frame $\vec{r}_{cg0}$, is defined as:

$$\vec{r}_{cg0} = \frac{1}{m}\iiint_V \rho(\vec{r}_0 + \vec{r})\, dV = \frac{1}{m}\widetilde{\underline{I}}^T \cdot \underline{M} \cdot \overline{r}_{bi} = \vec{r}_0 + \frac{1}{m}\widetilde{\underline{I}}^T \cdot \underline{M} \cdot \overline{r}_b \tag{9}$$

from which, the CG location with respect to the Local frame's origin can be computed as:

$$\vec{r}_{cg} = \vec{r}_{cg0} - \vec{r}_0 = \frac{1}{m}\widetilde{\underline{I}}^T \cdot \underline{M} \cdot \overline{r}_b \tag{10}$$

[3]For vectors $\vec{a}$ and $\vec{b}$, where $\underline{A}$ and $\underline{B}$ are their respective skew-symmetric representations, we can use the following relations: $\vec{a} \times \vec{b} = \underline{A} \cdot \vec{b} = -\underline{B} \cdot \vec{a}$

### 2.2 Stiffness Model

The stiffness matrix **K** is derived from a finite element analysis. Unlike the diagonal mass matrix, the stiffness matrix does change with elastic deformation.

The following constraints must be met

$$\widetilde{\underline{I}}^T \cdot \underline{K} \cdot \overline{u}_e = 0 \qquad \underline{R}_b \cdot \underline{K} \cdot \overline{u}_e = 0 \tag{11}$$

implying that the elastic forces, caused by stiffness, are internal forces, resulting in zero net forces and moments about the origin.

### 2.3 Kinematic Model

We define $\vec{V}_0$ as the velocity of the Local frame's origin with respect to the Inertial frame. The Local frame can be rotated from the Inertial frame via Euler Angles, $\phi, \theta, \psi$, and the Direction Cosine Matrix, $\underline{T}_{DCM}$, therefore

$$\vec{V}_0 = \frac{d\vec{r}_0}{dt} = \begin{bmatrix} u \\ v \\ w \end{bmatrix} = \underline{T}_{DCM}(\phi, \theta, \psi) \cdot \begin{bmatrix} \dot{x}_0 \\ \dot{y}_0 \\ \dot{z}_0 \end{bmatrix} \tag{12}$$

where $x_0, y_0$, and $z_0$ are the Inertial coordinates of the Local frame origin, and $\dot{x}_0, \dot{y}_0, \dot{z}_0$ and $u, v, w$ are the velocities of the Local frame origin in the Inertial and Local frames, respectively. The Direction Cosine Matrix ($\underline{T}_{DCM}$) is defined as:

$$\underline{T}_{DCM}(\phi, \theta, \psi) = \begin{bmatrix} c(\theta)c(\psi) & \begin{matrix} s(\phi)s(\theta)c(\psi) \\ - c(\phi)s(\psi) \end{matrix} & \begin{matrix} c(\phi)s(\theta)c(\psi) \\ + s(\phi)s(\psi) \end{matrix} \\ c(\theta)s(\psi) & \begin{matrix} s(\phi)s(\theta)s(\psi) \\ + c(\phi)c(\psi) \end{matrix} & \begin{matrix} c(\phi)s(\theta)s(\psi) \\ - s(\phi)c(\psi) \end{matrix} \\ -s(\theta) & s(\phi)c(\theta) & c(\phi)c(\theta) \end{bmatrix} \tag{13}$$

where $s$ and $c$ stand for the sine and cosine operators.

$\vec{\omega} = \begin{bmatrix} p & q & r \end{bmatrix}^T$ is the rotational velocity vector of the Local frame with respect to the Inertial frame, where $p$, $q$, and $r$ are the angular velocities of the vehicle about its Local axes $x$, $y$, and $z$, respectively. $\underline{\Omega}$ is the skew-symmetric representation of the angular velocity vector, and $\widetilde{\underline{\Omega}} \in \mathbb{R}^{3N \times 3N}$ is the block-diagonal extension of $\underline{\Omega}$, defined as:

$$\underline{\Omega} = \begin{bmatrix} 0 & -r & q \\ r & 0 & -p \\ -q & p & 0 \end{bmatrix} \qquad \widetilde{\underline{\Omega}} = \begin{bmatrix} \underline{\Omega} & \underline{0} & \underline{0} & \underline{0} \\ \underline{0} & \underline{\Omega} & \underline{0} & \underline{0} \\ \underline{0} & \underline{0} & \ddots & \underline{0} \\ \underline{0} & \underline{0} & \underline{0} & \underline{\Omega} \end{bmatrix} \tag{14}$$

### 2.4 Inertial Derivatives

The time derivative [4] of the discrete position vector of the deformed structure with respect to the Inertial frame is:

$$\frac{d\overline{r}_{bi}}{dt} = \widetilde{\underline{I}} \cdot \frac{d\vec{r}_0}{dt} + \frac{d\overline{r}_b}{dt} = \widetilde{\underline{I}} \cdot \vec{V}_0 + \dot{\overline{r}}_b + \widetilde{\underline{\Omega}} \cdot \overline{r}_b \tag{15}$$

[4] Note that the notation $\frac{d()}{dt}$ is used to represent the time derivative with respect to the Inertial frame, while $\dot{()}$ is used to represent the time derivative with respect to the Body frame (i.e., the relative time derivative).

where $\dot{\overline{r}}_b$ is the velocity vector of the deformed grids with respect to the Body frame.

Note that

$$\underline{\tilde{\Omega}} \cdot \overline{r}_b = -\underline{R}_b \cdot \vec{\omega} \tag{16}$$

where both terms stand for the cross product of $\vec{\omega} \times \vec{r}$ when using the discrete nodes position vector $\overline{r}_b$. Throughout the derivation, we use $\underline{\tilde{\Omega}} \cdot \overline{r}_b$ and $-\underline{R}_b \cdot \vec{\omega}$ interchangeably.

Since $\dot{\overline{r}}_{b0} = 0$, eq. 15 becomes:

$$\frac{d\overline{r}_{bi}}{dt} = \underline{\widetilde{I}} \cdot \vec{V}_0 + \dot{\overline{u}}_e + \underline{\widetilde{\Omega}} \cdot \overline{r}_b = \underbrace{\underline{\widetilde{I}} \cdot \vec{V}_0 + \underline{\widetilde{\Omega}} \cdot \overline{r}_{b0}}_{\text{rigid velocity terms}} + \underbrace{\dot{\overline{u}}_e + \underline{\widetilde{\Omega}} \cdot \overline{u}_e}_{\text{elastic velocity terms}} \tag{17}$$

The acceleration vector of the deformed structure with respect to the Inertial frame is:

$$\frac{d^2\overline{r}_{bi}}{dt^2} = \underbrace{\underline{\widetilde{I}} \cdot \dot{\vec{V}}_0 + \underline{\dot{\widetilde{\Omega}}} \cdot \overline{r}_{b0} + \underline{\widetilde{\Omega}} \cdot (\underline{\widetilde{I}} \cdot \vec{V}_0 + \underline{\widetilde{\Omega}} \cdot \overline{r}_{b0})}_{\text{rigid acceleration terms}} + \underbrace{\ddot{\overline{u}}_e + \underline{\dot{\widetilde{\Omega}}} \cdot \overline{u}_e + 2\underline{\widetilde{\Omega}} \cdot \dot{\overline{u}}_e + \underline{\widetilde{\Omega}} \cdot \underline{\widetilde{\Omega}} \cdot \overline{u}_e}_{\text{elastic acceleration terms}} \tag{18}$$

### 2.5 EOM Derivation From Newton's Second Law

The *linear momentum* vector of all points on the deformed grid with respect to the Inertial frame, $\overline{p}_{bi}$, the *total linear momentum* of all points on the deformed grid with respect to the Inertial frame, $\vec{P}_0$, and the *total angular momentum* of all points on the deformed grid with respect to the Inertial frame, about the Local frame origin, $\vec{H}_0$, are provided by:

$$\begin{aligned}
\overline{p}_{bi} =& \underline{M} \cdot \frac{d\overline{r}_{bi}}{dt} = \underline{M} \cdot \left( \underline{\widetilde{I}} \cdot \vec{V}_0 + \dot{\overline{u}}_e - \underline{R}_b \cdot \vec{\omega} \right) \\
\vec{P}_0 =& \underline{\widetilde{I}}^T \cdot \underline{M} \cdot \left( \underline{\widetilde{I}} \cdot \vec{V}_0 + \dot{\overline{u}}_e - \underline{R}_b \cdot \vec{\omega} \right) = m\vec{V}_0 + \underline{\widetilde{I}}^T \cdot \underline{M} \cdot \dot{\overline{u}}_e - m\vec{r}_{cg} \times \vec{\omega} \\
\vec{H}_0 =& -\underline{R}_b^T \cdot \underline{M} \cdot \left( \underline{\widetilde{I}} \cdot \vec{V}_0 + \dot{\overline{u}}_e - \underline{R}_b \cdot \vec{\omega} \right) = \underline{I}_M \cdot \vec{\omega} - \underline{R}_b^T \cdot \underline{M} \cdot \dot{\overline{u}}_e + m\vec{r}_{cg} \times \vec{V}_0
\end{aligned} \tag{19}$$

The nonlinear EOM are derived by applying Newton's second law

$$\begin{aligned}
\frac{d\overline{p}_{bi}}{dt} =& \overline{F}_{ex} + \underline{M} \cdot \underline{\widetilde{I}} \cdot \vec{g} - \underline{K} \cdot \overline{u}_e \\
\frac{d\vec{P}_0}{dt} =& \underline{\widetilde{I}}^T \cdot \overline{F}_{ex} + m\vec{g} \\
\frac{d\vec{H}_0}{dt} =& -\underline{R}_b^T \cdot \overline{F}_{ex}
\end{aligned} \tag{20}$$

where $\overline{F}_{ex}$ is the external load vector (due to aerodynamics, thrust, etc.) and $\vec{g}$ is the gravity acceleration vector.

The full EOM derivation using Eqs. 20 and 19 is detailed in Appendix A. Hereafter we analyze the coupled dynamics in *Body Axes* with the origin at the instantaneous floating CG and axes following the body's rotation. I.e., the *Local frame* is a *Body frame* (see Appendix A for a detailed discussion of the different frames). The resulting set of EOM in Body frame is

$$\begin{bmatrix} m\underline{I} & \underline{0} & \underline{0} \\ \underline{0} & \underline{I}_M & -\underline{R}_b^T \cdot \underline{M} \\ \underline{M} \cdot \underline{\widetilde{I}} & -\underline{M} \cdot \underline{R}_b & \underline{M} \end{bmatrix} \cdot \begin{bmatrix} \dot{\vec{V}}_0 \\ \dot{\vec{\omega}} \\ \ddot{\overline{u}}_e \end{bmatrix} = \begin{bmatrix} \overrightarrow{RHS}_T \\ \overrightarrow{RHS}_R \\ \overrightarrow{RHS}_E \end{bmatrix} \tag{21}$$

where [5]:

$$\begin{aligned}
\overrightarrow{RHS}_T &= -m\vec{\omega} \times \vec{V}_0 + \underline{\widetilde{I}}^T \cdot \overline{F}_{ex} + m\vec{g} \\
\overrightarrow{RHS}_R &= -\vec{\omega} \times \left(\underline{I}_M \cdot \vec{\omega} - \underline{R}_b^T \cdot \underline{M} \cdot \dot{\overline{u}}_e\right) - \underline{\dot{I}}_M \cdot \vec{\omega} + \underline{\dot{R}}_b^T \cdot \underline{M} \cdot \dot{\overline{u}}_e - \underline{R}_b^T \cdot \overline{F}_{ex} \\
\overrightarrow{RHS}_E &= -\left(\underline{M} \cdot \underline{\widetilde{\Omega}} + \underline{\widetilde{\Omega}} \cdot \underline{M}\right) \cdot \dot{\overline{u}}_e - \underline{\widetilde{\Omega}} \cdot \underline{M} \cdot \underline{\widetilde{I}} \cdot \vec{V}_0 - \underline{\widetilde{\Omega}} \cdot \underline{M} \cdot \underline{\widetilde{\Omega}} \cdot \vec{r}_b \\
&\quad + \overline{F}_{ex} + \underline{M} \cdot \underline{\widetilde{I}} \cdot \vec{g} - \underline{K} \cdot \overline{u}_e
\end{aligned} \tag{22}$$

The equation sets are strongly coupled through the acceleration terms, implying that neither set can be solved separately, even if the full state is known. In eq. 21, it is evident that while the translational and rotational equation sets are lightly coupled (only via non-acceleration terms on the RHS), both are strongly coupled with the elastic equation set.

### 2.6 EOM Terms Investigation

To gain insight into the nonlinear dynamics, each coupling term in equation set 21 is analyzed individually. We assess the impact of the coupling terms on the overall forces, moments, and elastic out-of-plane ($z$-direction) acceleration. This includes considering the effects of flight velocity (mainly in the $x$ direction), rotational motion about all three axes ($\vec{\omega} = [p, q, r]^T$), and both small and large deformations in the $z$-direction. To simplify the investigation we assume that the in-plane elastic deformations are negligible (namely, $\overline{u}_e = [0, 0, u_z]^T$), and that the elastic deformation is harmonic, $u_z = A(y) \cdot sin(\omega_n t)$. Furthermore, we assume that wing dimensions in the y direction are the largest (namely, $\overline{r}_b = [0, y, u_z]^T$).

For this investigation only, we examine the effect of a single element:

$$\underline{\widetilde{\Omega}} = \begin{bmatrix} 0 & -r & q \\ r & 0 & -p \\ -q & p & 0 \end{bmatrix} \qquad \underline{M} = \begin{bmatrix} m & 0 & 0 \\ 0 & m & 0 \\ 0 & 0 & m \end{bmatrix} \qquad \underline{R}_b = \begin{bmatrix} 0 & -u_Z & y \\ u_Z & 0 & -0 \\ -y & 0 & 0 \end{bmatrix} \tag{23}$$

Finally, the elastic terms are investigated as forcing terms on the rigid and elastic dynamics. That is, their sign reflects their effect on the RHS of eq. 21.

**CG Rotational EOM.**

- $\underline{R}_b^T \cdot \underline{M} \cdot \ddot{\overline{u}}_e$ can be interpreted as the elastic contribution to the aircraft's angular inertia. It can be approximated as:

$$\underline{R}_b^T \cdot \underline{M} \cdot \ddot{\overline{u}}_e = -m\omega_n^2 \begin{bmatrix} 0 \\ -y \\ -u_z \end{bmatrix} \times \begin{bmatrix} 0 \\ 0 \\ u_z \end{bmatrix} = m\omega_n^2 y u_z \hat{x} \tag{24}$$

  A symmetric bending acceleration will have a zero net effect when integrated over the two wings. An anti-symmetric bending acceleration will cause a rigid roll moment in the bending direction (opposite the acceleration direction) that will preserve the angular momentum.
- $-\underline{\dot{I}}_M \cdot \vec{\omega}$ is a term due to inertia time-variation that may also exist in rigid aircraft dynamics due to fuel consumption, for example. The moment of inertia matrix and its time

[5] Subscript T denotes translational motion, R denotes rotational motion, and E denotes elastic motion.

derivative are defined as:

$$\begin{aligned}\underline{I}_M &= \begin{bmatrix} \iiint_V \rho(y^2+z^2)\,dV & \iiint_V -\rho(xy)\,dV & \iiint_V -\rho(xz)\,dV \\ \iiint_V -\rho(xy)\,dV & \iiint_V \rho(x^2+z^2)\,dV & \iiint_V -\rho(yz)\,dV \\ \iiint_V -\rho(xz)\,dV & \iiint_V -\rho(yz)\,dV & \iiint_V \rho(x^2+y^2) \end{bmatrix} \\ \dot{\underline{I}}_M &= \begin{bmatrix} \iiint_V \rho(2y\dot{y}+2z\dot{z})\,dV & \iiint_V -\rho(x\dot{y}+y\dot{x})\,dV & \iiint_V -\rho(x\dot{z}+z\dot{x})\,dV \\ \iiint_V -\rho(x\dot{y}+y\dot{x})\,dV & \iiint_V \rho(2x\dot{x}+2z\dot{z})\,dV & \iiint_V -\rho(y\dot{z}+z\dot{y})\,dV \\ \iiint_V -\rho(x\dot{z}+z\dot{x})\,dV & \iiint_V -\rho(y\dot{z}+z\dot{y})\,dV & \iiint_V \rho(2y\dot{y}+2x\dot{x})\,dV \end{bmatrix} \end{aligned} \tag{25}$$

In elastic motion, the largest $\dot{\underline{I}}_M$ element is $\dot{I}_{yz} \approx \iiint_V \rho(y\dot{z})\,dV$, which is nonzero only in anti-symmetric bending. This term is an addition to the gyroscopic effect ($\vec{\omega} \times (\underline{I}_M \cdot \vec{\omega})$), where a yawing motion creates pitch acceleration and a pitching motion creates a yaw acceleration, in anti-symmetric bending deformation only. Integrated over both wings in symmetric deformation, these moments cancel each other out.

- $\vec{\omega} \times \left(\underline{R}_b^T \cdot \underline{M} \cdot \dot{\overline{u}}_e\right)$ can be approximated as:

$$\vec{\omega} \times \left(\underline{R}_b^T \cdot \underline{M} \cdot \dot{\overline{u}}_e\right) = m \begin{bmatrix} p \\ q \\ r \end{bmatrix} \times \left( \begin{bmatrix} 0 \\ -y \\ -u_z \end{bmatrix} \times \begin{bmatrix} 0 \\ 0 \\ \omega_n u_z \end{bmatrix} \right) = m\omega_n y u_z \left(-r\hat{y} + q\hat{z}\right) \tag{26}$$

  It is evident that this term is another elastic contribution to the gyroscopic effect, where, in anti-symmetric bending deformation, a yawing motion creates a pitching moment, and a pitching motion creates a yawing moment. Both moments are proportional to $myu_z$ and therefore can be interpreted as $\dot{I}_{yz}$ terms, implying that both this and previous term are stabilizing terms. Using Eq. 26, the stabilizing effect can be described as follows: An increase in the pitch rate leads to an increased yawing moment, resulting in an increased yaw rate that, in turn, generates a negative pitching moment, leading to a decrease in the pitch rate.
- $\dot{\underline{R}}_b^T \cdot \underline{M} \cdot \dot{\overline{u}}_e$ is a second order term in elastic deformation rates (recall that $\dot{\vec{r}}_b = \dot{\overline{u}}_e$). This term has a small contribution to angular acceleration, as it is the cross-product of almost parallel terms. This second-order term is neglected in linear elasticity.

**Elastic EOM.** The elastic EOM consists mainly of the five factors that contribute to inertial acceleration: Origin's translation acceleration, relative acceleration, Coriolis acceleration, translational acceleration due to angular acceleration, and centrifugal acceleration.

- $-\widetilde{\underline{\Omega}} \cdot \underline{M} \cdot \widetilde{\underline{\Omega}} \cdot \overline{r}_b$ -This term has two contributions, (since $\overline{r}_b = \overline{r}_{b0} + \overline{u}_e$). Both represent the elastic acceleration due to centrifugal acceleration.
  - $-\widetilde{\underline{\Omega}} \cdot \underline{M} \cdot \widetilde{\underline{\Omega}} \cdot \overline{r}_{b0}$ can be approximated as:

$$-\widetilde{\underline{\Omega}} \cdot \underline{M} \cdot \widetilde{\underline{\Omega}} \cdot \overline{r}_{b0} = -m \begin{bmatrix} p \\ q \\ r \end{bmatrix} \times \left( \begin{bmatrix} p \\ q \\ r \end{bmatrix} \times \begin{bmatrix} 0 \\ y \\ 0 \end{bmatrix} \right) = m \begin{bmatrix} qpy \\ (p^2+r^2)y \\ -rqy \end{bmatrix} \approx m \begin{bmatrix} 0 \\ (p^2+r^2)y \\ 0 \end{bmatrix} \tag{27}$$

    The bending moment (positive for upward bending) this term generates is $-m(p^2+r^2)y^2u_z$, which means during yaw or roll motion, any elastic motion would generate a stabilizing bending moment (similar to the stabilizing bending moment in rotating wing's dynamics).
  - $-\widetilde{\underline{\Omega}} \cdot \underline{M} \cdot \widetilde{\underline{\Omega}} \cdot \overline{u}_e$ can be approximated as:

$$-\widetilde{\underline{\Omega}} \cdot \underline{M} \cdot \widetilde{\underline{\Omega}} \cdot \overline{u}_e = -m \begin{bmatrix} p \\ q \\ r \end{bmatrix} \times \left( \begin{bmatrix} p \\ q \\ r \end{bmatrix} \times \begin{bmatrix} 0 \\ y \\ 0 \end{bmatrix} \right) = -m \begin{bmatrix} rpu_z \\ rquZ \\ -(p^2+q^2)u_z \end{bmatrix} \approx m \begin{bmatrix} 0 \\ 0 \\ (p^2+q^2)u_z \end{bmatrix} \tag{28}$$

This term can destabilizing the bending motion while the aircraft is in pitching or rolling motions. The force is proportional to the bending deformation, thus it is a negative stiffness term. Adding this term to the structural stiffness we get: $\underline{K} \cdot \overline{u}_e + \underline{\widetilde{\Omega}} \cdot \underline{M} \cdot \underline{\widetilde{\Omega}} \cdot \overline{u}_e = m\omega_n^2 \left(1 - \frac{q^2+p^2}{\omega_n^2}\right) u_z$, indicating that this term is significant when the ratio between the angular rates and the natural frequency is non-negligible.

- $-\left(\underline{M} \cdot \underline{\widetilde{\Omega}} + \underline{\widetilde{\Omega}} \cdot \underline{M}\right) \cdot \dot{\overline{u}}_e$ is the elastic force due to Coriolis accelerations. This term does not have an out-of-plane acceleration component due to out-of-plane deformation rates; thus, it has a very small contribution to the elastic EOM.
- $-\underline{M} \cdot \underline{\widetilde{I}} \cdot \dot{\vec{V}}_0 - \underline{\widetilde{\Omega}} \cdot \underline{M} \cdot \underline{\widetilde{I}} \cdot \vec{V}_0$ is the elastic force due to the CG's total translational acceleration. This term might have a significant impact during maneuvers involving z-direction CG acceleration and a high pitching rate.
- $\underline{M} \cdot \underline{R}_b \cdot \dot{\vec{\omega}}$ is the elastic force due to the CG's rotational acceleration. This term has two parts, rigid and elastic (since $\overline{r}_b = \overline{r}_{b0} + \overline{u}_e$). The rigid term might have a significant impact during roll acceleration, while the z-direction elastic deformations do not generate z-direction elastic accelerations.

The flight-dynamics-aeroelastic coupling effects discussed above depend on the elastic deformation magnitude (small/large) and on the maneuver intensity (light/hard). They are pronounced in cases of flexible vehicles that undergo significant deformations during hard maneuvers. Table 1 lists the substantial coupling effects and provides their magnitudes as a function of the out-of-plane elastic deformations, $u_z$, the frequency of the aeroelastic first symmetric bending mode, $\omega_n$,[6] the aircraft wing span, $b$, and the maneuver rates and accelerations. Table 1 does not include the mass and inertia variation terms discussed above.

| Term | Impact | Magnitude |
|---|---|---|
| $\underline{R}_b^T \cdot \underline{M} \cdot \ddot{\overline{u}}_e$ | rolling moment | $m\omega_n^2 y u_z$ |
| $\vec{\omega} \times \left(\underline{R}_b^T \cdot \underline{M} \cdot \dot{\overline{u}}_e\right)$ | pitching moment | $mbr\omega_n u_z$ |
| | yawing moment | $mbq\omega_n u_z$ |
| $\dot{\underline{I}}_M \cdot \vec{\omega}$ | pitching moment | $mbr\omega_n u_z$ |
| | yawing moment | $mbq\omega_n u_z$ |
| $\underline{M} \cdot \underline{\widetilde{I}} \cdot \dot{\vec{V}}_0$ | elastic loads | $mgn_z$ |
| $\underline{\widetilde{\Omega}} \cdot \underline{M} \cdot \underline{\widetilde{I}} \cdot \vec{V}_0$ | elastic loads | $mqV$ |
| $\underline{M} \cdot \underline{R}_b \cdot \dot{\vec{\omega}}$ | elastic loads | $mb\dot{p}$ |
| $\underline{\widetilde{\Omega}} \cdot \underline{M} \cdot \underline{\widetilde{\Omega}} \cdot \overline{r}_{b0}$ | internal bending moment | $m(p^2+r^2)b^2 u_z$ |
| $\underline{K} \cdot \overline{u}_e + \underline{\widetilde{\Omega}} \cdot \underline{M} \cdot \underline{\widetilde{\Omega}} \cdot \overline{u}_e$ | elastic stiffness | $m\omega_n^2 \left(1 - \frac{q^2+p^2}{\omega_n^2}\right) u_z$ |

Table 1: Flight-dynamics-aeroelastic coupling effects and their magnitudes

[6]The frequency of the first bending mode does not change significantly with airspeed. It also does not change much with elastic deformations (see, for example, in the case of the very flexible Pazy wing [14]). Thus, the first bending natural frequency can be used as an approximation of the aeroelastic frequency of the deformed wing to estimate the magnitude of the stiffness terms.

## 3 LINEARIZED MODEL AND MODAL REPRESENTATION

For stability analysis about an equilibrium state, the nonlinear EOM (eq. 21) are linearized. Traditionally, stability analysis is partitioned into rigid body stability and flutter analysis, which are performed independently. In the following, we propose a linearized formulation, using generalized coordinates, that can be used to solve the coupled rigid-body-elastic stability problem.

For the linearization, we define a nominal equilibrium state by the position of each DOF,

$$\overline{r}_{bi}^{n} = \widetilde{\underline{I}} \cdot \vec{r}_0^{n} + \overline{r}_{b0}^{n} + \overline{u}_e^{n} \tag{29}$$

which is determined from the solution of the nonlinear EOM (eq. 21) in a steady state.[7] Assuming small disturbances about the nominal state, the perturbation in the DOFs' positions can be described as a linear superposition of rigid and elastic mode shapes:[8]

$$\delta\overline{r}_{bi} = \overline{r}_{bi} - \overline{r}_{bi}^{n} = \underline{\Phi} \cdot \overline{\xi} \tag{30}$$

where $\underline{\Phi} \in \mathbb{R}^{3N \times N_m}$ is the modes matrix, holding the set of $N_m$ structural modes, computed as the eigenvectors of the undamped, unforced system, and $\overline{\xi} \in \mathbb{R}^{N_m \times 1}$ is the modal participation vector. For a free aircraft configuration, the modes matrix and the modal participation vector can be split into rigid-body and elastic components, as:

$$\underline{\Phi} = \begin{bmatrix} \underline{\Phi}_r & \underline{\Phi}_e \end{bmatrix} \qquad \overline{\xi} = \begin{bmatrix} \overline{\xi}_r \\ \overline{\xi}_e \end{bmatrix} \tag{31}$$

From eq. 30 each component can be written as:

$$\begin{aligned} \delta\vec{r}_0 &= \vec{r}_0 - \vec{r}_0^{n} \\ \delta\overline{r}_{b0} &= \overline{r}_{b0} - \overline{r}_{b0}^{n} = \left(\underline{\delta\tilde{\Theta}} - \widetilde{\underline{I}}\right) \cdot \overline{r}_{b0}^{n} \\ \delta\overline{u}_e &= \overline{u}_e - \overline{u}_e^{n} \end{aligned} \tag{32}$$

where $\widetilde{\underline{I}} \in \mathbb{R}^{3N \times 3N}$ is the block-diagonal extension of the identity matrix. $\underline{\delta\tilde{\Theta}} \in \mathbb{R}^{3N \times 3N}$ is the block-diagonal extension of the rotation matrix from the nominal body axes to the actual body axes, defined as:

$$\underline{\delta\Theta} = \underline{T}_{DCM}(\phi, \theta, \psi) \cdot \underline{T}_{DCM}^{T}(\phi^n, \theta^n, \psi^n) \qquad \underline{\delta\tilde{\Theta}} = \begin{bmatrix} \underline{\delta\Theta} & \underline{0} & \underline{0} & \underline{0} \\ \underline{0} & \underline{\delta\Theta} & \underline{0} & \underline{0} \\ \underline{0} & \underline{0} & \ddots & \underline{0} \\ \underline{0} & \underline{0} & \underline{0} & \underline{\delta\Theta} \end{bmatrix} \tag{33}$$

For small angular disturbances, $(\underline{\delta\Theta} - \underline{\mathrm{I}})$ can be written as the skew-symmetric representation of a physical vector $\delta\vec{\vartheta}$, defined next.

Using the modal representation, we get:

$$\begin{aligned} \underline{\Phi}_e \cdot \overline{\xi}_e &= \delta\overline{u}_e & \qquad \underline{\Phi}_r \cdot \overline{\xi}_r &= \widetilde{\underline{I}} \cdot \delta\vec{r}_0 + \delta\overline{r}_{b0} \\ \delta\vec{r}_0 &= \underline{D}_T \cdot \underline{\Phi}_r \cdot \overline{\xi}_r & \qquad \delta\vec{\vartheta} &= \underline{D}_R \cdot \underline{\Phi}_r \cdot \overline{\xi}_r \end{aligned} \tag{34}$$

[7] Note that all vectors in this section are presented in the body frame of the nominal state.

[8] Note that this holds even for large nominal deformations.

Since the set of rigid body modes, $\underline{\Phi}_r$, computed in a FE software typically comprises coupled translation-rotation motions, $\underline{D}_T \in \mathbb{R}^{3\times 3N}$ and $\underline{D}_R \in \mathbb{R}^{3\times 3N}$ are transformation matrices used to extract the clean unit translation/rotation rigid body modes from $\underline{\Phi}_r$. They are defined as

$$\underline{D}_T = \begin{bmatrix} \underline{I} & \underline{0} \end{bmatrix} \cdot \left(\underline{\Phi}_r^{synt}\right)^{\dagger} \qquad \underline{D}_R = \begin{bmatrix} \underline{0} & \underline{I} \end{bmatrix} \cdot \left(\underline{\Phi}_r^{synt}\right)^{\dagger} \tag{35}$$

where $\underline{\Phi}_r^{synt} \in \mathbb{R}^{3N\times 6}$ is a matrix of synthetically-defined six rigid body modes, each mode defined by a unit displacement/rotation of the origin in a single DOF and zero displacement/rotation of the others, and the displacement/rotation at all other nodes are computed from kinematic relations. Matrix $\underline{\Phi}_r^{synt}$ comprises six modes, each representing a unit translation in the $x, y,$ or $z$ directions of the body's frame at the nominal state or a unit rotation about one of these axes. Since $\underline{\Phi}_r^{synt}$ is not a square matrix, the superscript "†" in eq. 35 denotes the pseudo inverse.

### *3.0.1 EOM in Modal Coordinates*

The modal represetation of the perturbations, defined in the previous section, are used to derive the linearized EOM, in modal coordinates:

$$\begin{aligned} &\underline{M}\cdot\underline{\Phi}_r\cdot\ddot{\underline{\xi}}_r + \underline{M}\cdot\underline{\Phi}_e\cdot\ddot{\underline{\xi}}_e + \left(\widetilde{\underline{\Omega}}^n\cdot\underline{M} - \underline{M}\cdot\widetilde{\underline{\Omega}}^n\right)\cdot\underline{\Phi}_r\cdot\dot{\underline{\xi}}_r \\ &+ \left(\widetilde{\underline{\Omega}}^n\cdot\underline{M} - \underline{M}\cdot\widetilde{\underline{\Omega}}^n\right)\cdot\underline{\Phi}_e\cdot\dot{\underline{\xi}}_e + \delta\widetilde{\underline{\Omega}}\cdot\underline{M}\cdot\left(\widetilde{\underline{I}}\cdot\vec{V}_0^n + \widetilde{\underline{\Omega}}^n\cdot\overline{r}_b^n\right) \\ &+ \widetilde{\underline{\Omega}}^n\cdot\underline{M}\cdot\delta\widetilde{\underline{\Omega}}\cdot\overline{u}_e^n + \widetilde{\underline{\Omega}}^n\cdot\underline{M}\cdot\widetilde{\underline{\Omega}}^n\cdot\delta\overline{r}_{b0} + \underline{K}\cdot\underline{\Phi}_e\cdot\overline{\xi}_e = \overline{F}_{ex} \end{aligned} \tag{36}$$

The full derivation is presented in Appendix B.

A significant simplification of the EOM is achieved by taking advantage of the orthogonality of the modes. Pre-multiply eq. 36 by the modes matrix transposed and assigning the relations

$$\delta\overline{r}_{b0} = -\underline{R}_{b0}^n\cdot\underline{D}_R\cdot\underline{\Phi}_r\cdot\overline{\xi}_r \tag{37}$$

$$\delta\vec{\omega} = \frac{d}{dt}\delta\vec{\vartheta} = \underline{D}_R\cdot\underline{\Phi}_r\cdot\dot{\overline{\xi}}_r \tag{38}$$

yields the coupled disturbances EOM in modal coordinates representation:

$$\underline{GM}\cdot\ddot{\overline{\xi}} + \underline{GC}\cdot\dot{\overline{\xi}} + \underline{G\Omega}\cdot\dot{\overline{\xi}} + \underline{GP}\cdot\dot{\overline{\xi}} + \underline{GU}\cdot\dot{\overline{\xi}} + \underline{GR}\cdot\overline{\xi} + \underline{GK}\cdot\overline{\xi} = \overline{GF}_{ex} \tag{39}$$

where [9]

$$\begin{aligned} \underline{GM} &= \underline{\Phi}^T\cdot\underline{M}\cdot\underline{\Phi} \qquad \underline{GC} = 2\underline{GM}\cdot\overline{\zeta}\odot\overline{\omega}_n \qquad \underline{GK} = \underline{\Phi}^T\cdot\underline{K}\cdot\underline{\Phi} \qquad \overline{GF} = \underline{\Phi}^T\cdot\overline{F}_{ex} \\ \underline{G\Omega} &= \underline{\Phi}^T\cdot\left(\widetilde{\underline{\Omega}}^n\cdot\underline{M} - \underline{M}\cdot\widetilde{\underline{\Omega}}^n\right)\cdot\underline{\Phi} \qquad \underline{GP} = -\underline{\Phi}^T\cdot\underline{R}_{pbi}^n\cdot\underline{D}_R\cdot\underline{\Phi}\cdot\underline{I}_r \\ \underline{GR} &= -\underline{\Phi}^T\cdot\underline{\Omega}^n\cdot\underline{M}\cdot\underline{\Omega}^n\cdot\underline{R}_{b0}^n\cdot\underline{D}_R\cdot\underline{\Phi}\cdot\underline{I}_r \qquad \underline{GU} = -\underline{\Phi}^T\cdot\underline{\Omega}^n\cdot\underline{M}\cdot\underline{R}_{ue}^n\cdot\underline{D}_R\cdot\underline{\Phi}\cdot\underline{I}_r \end{aligned} \tag{40}$$

The generalized damping matrix $\underline{GC}$ was added to introduce structural damping. $\overline{\zeta}$ and $\overline{\omega}_n$ are the modal damping and frequency vectors, respectively, whose elements are the modal damping and natural frequency values of each mode. Typical values of $\zeta_i$ are in the order of 0.01 but

[9] Note that if the dynamic model (i.e. $\underline{M}, \underline{K}$ and $\underline{\Phi}$ matrices) is not constructed in the Body frame's orientation, these matrices should be rotated using a rotation matrix from the dynamic model coordinate frame to the Body frame.

may vary for each elastic mode. $\underline{R}^n_{b0}$ is defined in Appendix B. $\underline{R}^n_{ue} \in \mathbb{R}^{3N\times 3}$ is the skew-symmetric representation of the nominal elastic deformation vector $\overline{u}^n_e$ (similar definition to $\underline{R}_b$, as in eq.8). $\underline{R}^n_{pbi} \in \mathbb{R}^{3N\times 3}$ is the skew-symmetric representation of the linear momentum (with respect to inertial frame) of each node in the nominal state $\overline{p}^n_{bi} = \underline{M} \cdot \left(\widetilde{\underline{I}} \cdot \vec{V}^n_0 + \widetilde{\underline{\Omega}}^n \cdot \overline{r}^n_b\right)$. Finally, $\underline{I}_r \in \mathbb{R}^{N_m \times N_m}$ is a matrix that satisfy: $\underline{\Phi}_r \cdot \overline{\xi}_r = \underline{\Phi} \cdot \underline{I}_r \cdot \overline{\xi}$ defined as:

$$\underline{I}_r = \begin{bmatrix} \underline{\mathrm{I}} & \underline{0} & \underline{0} \\ \underline{0} & \underline{\mathrm{I}} & \underline{0} \\ \underline{0} & \underline{0} & \underline{0} \end{bmatrix} \tag{41}$$

In eq.39, the terms in black are those present in straight and level flight, as established in the literature, while the terms in red are the newly introduced coupling terms.

## 4 TEST CASE - THE ACTIVE AEROELASTIC AIRCRAFT TESTBED (A3TB)

The (Active Aeroelastic Aircraft Testbed (A3TB)), is a 3D-printed aeroelastic flight demonstrator. The flying-wing configuration has a geometry similar to that of the multi-utility aeroelastic demonstrator [15]. It is propelled by a pusher-propeller and electric engine. The wings are fitted with eight trailing-edge control surfaces for trim and aeroelastic response control. The A3TB was tested in flight demonstrating body-freedom flutter at [6]. The design is supported by high-fidelity aerodynamic, structural, and aeroelastic models, such that the A3TB can be further used for aeroelastic studies.

### 4.1 Models

Figure 2 shows the A3TB geometry. It is a flying wing configuration with three meters wingspan and constant chord of 0.3 meters. The rectangular wings are swept back in 22 degrees and twisted by negative 3 degrees (wash-out) from the wing root to the tip. A symmetric NACA-0012 airfoil was selected for its zero pitching moment coefficient. The wings have four trailing-edge control surfaces each, and wing-tip fins for increased lateral stability.

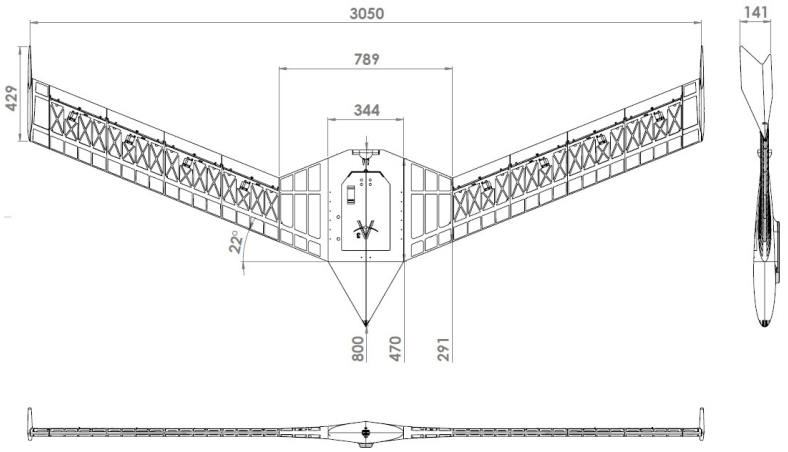


Figure 2: A3TB geometry

The A3TB structure is 3D-printed in segments from PA-12 Nylon material. The segments are connected via a 20x5 mm quasi-isotropic composite spar made of 22 carbon-fiber laminates.

The wings are wrapped in Oracover Polyester foil, providing the aerodynamic airfoil shape.

The full span A3TB structure was modeled in Nastran finite-element (FE) software using beam and plate elements, with a total of about 14K nodes and 16K elements in the GSET [16]. For stability analysis, the model was reduced to the ASET with 266 nodes, each with three translation DOFs. Figure 3 shows the FE model of the half airplane.

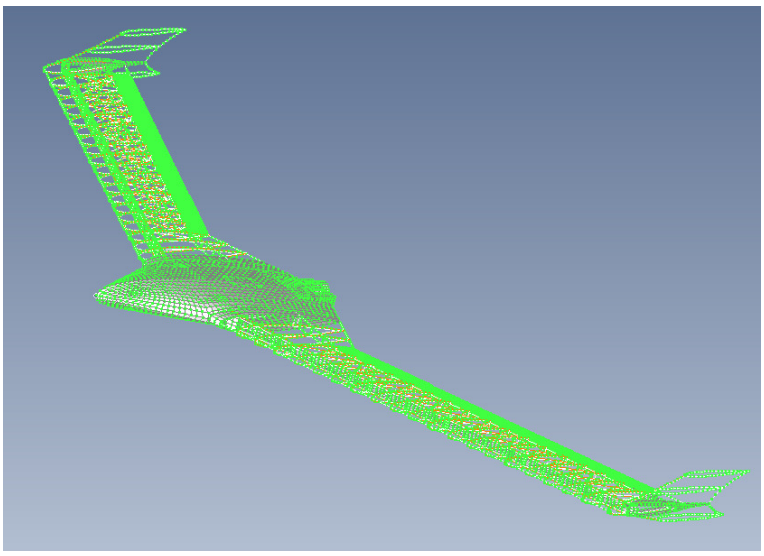

Figure 3: A3TB structural FE model

The A3TB Aerodynamic Influence Coefficient (AIC) matrix, $\underline{AIC}$, was computed in the ASET DOFs for the full-span airplane, using the ZAERO commercial software [11]. The Aerodynamic mesh contains 2450 panels (9800 nodes). Each section of the aircraft, including the body and winglets, was modeled as a thin lifting surface.

## 4.2 Analyses

### *4.2.1 Modal and Linear Stability Analyses*

The first four modes are shown in Table 2 and Figure 4 (in the aerodynamic panels). The model was calibrated in a ground vibration test, and each mode was characterized by close to zero modal damping.

| Elastic Mode | Description | Frequency [Hz] | Symmetry |
|---|---|---|---|
| #1 | first bending | 5.3 | symmetric |
| #2 | first torsion | 8.8 | anti-symmetric |
| #3 | first torsion | 10.8 | symmetric |
| #4 | second torsion | 11.7 | anti-symmetric |

Table 2: Elastic mode shapes classification and frequencies of the two configurations

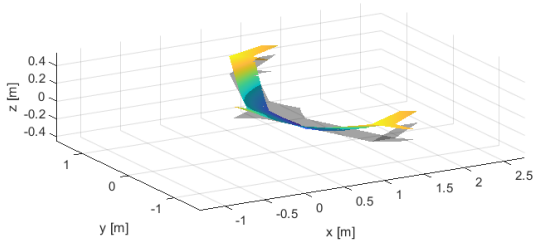


(a) Mode #1, $f = 5.3$ Hz

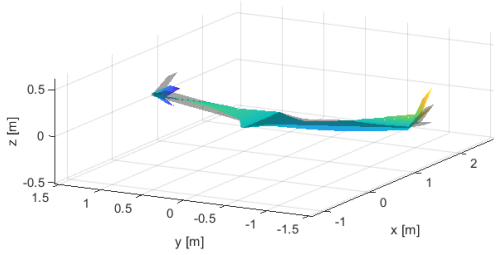


(b) Mode #2, $f = 8.8$ Hz

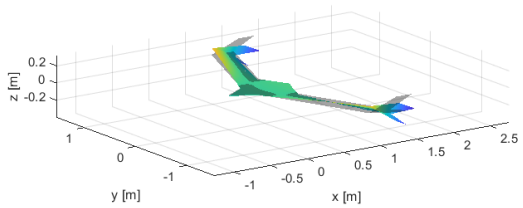


(c) Mode #3, $f = 10.8$ Hz

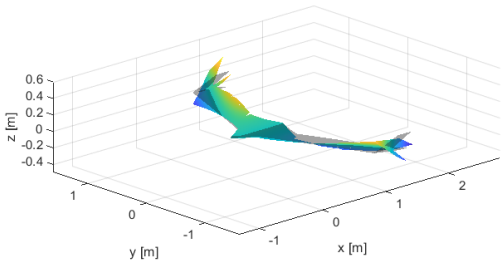


(d) Mode #4, $f = 11.7$ Hz

Figure 4: A3TB first four elastic modes in aerodynamic panels

Figure 5 shows an $\omega - V - g$ plot of the variation of aeroelastic frequencies and damping values with airspeed. The mode numbers are tracked and the flutter mechanisms are marked by the zero-damping crossings. The flutter analysis was performed using an in-house aeroelastic solver based on the PKH method [17], and mode tracking based on left and right eigenvectors [18]. The A3TB has three main flutter mechanisms, all are BFF type. S1 is the first symmetric flutter mechanism, which was verified in a dedicated flutter flight test [6]. This mechanism is characterized by sharp crossing and involves first bending and rigid pitch motions. The second mechanism, A1, is also a sharp crossing mechanism that involves anti-symmetric torsion and rigid roll motions. The third mechanism, S2, is a hump-mode mechanism that involves symmetric torsion and rigid pitch motions. The linear flutter analysis was performed about straight-and-level flight conditions accounting only for aeroelastic dynamics (i.e. without inertial coupling with rigid body dynamics). Note that all flutter mechanisms involve coupling with a rigid body mode (marked as mode 4 in Figure 5) comprising of pitch and roll motions.

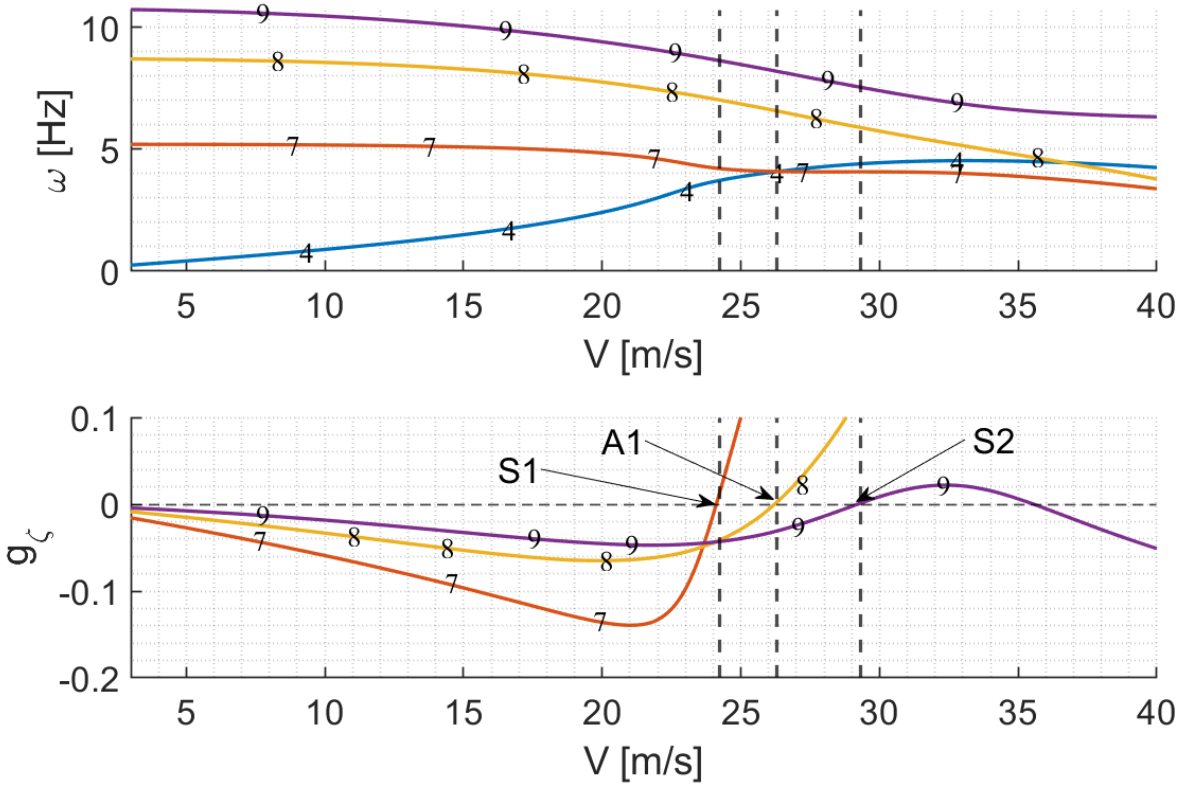


Figure 5: $\omega - V - g$ plot describing the aeroelastic frequencies and damping values as a function of airspeed; Computed at straight and level flight, $n = 1g$

### 4.3 Flutter Analysis in a Coordinated Turn

From the linearized EOM in modal coordinates (eq. 39) and assuming zero elastic deformations in the nominal state (i.e. $\overline{u}_e^n = 0$), we derive the coupled EOM of a maneuvering aircraft:

$$\underline{GM} \cdot \ddot{\overline{\xi}} + (\underline{GC} + \underline{G\Omega} + \underline{GP}) \cdot \dot{\overline{\xi}} + \left(\underline{GK} - \underline{Q}_{HH} + \underline{GR}\right) \cdot \overline{\xi} = 0 \tag{42}$$

where $\underline{Q}_{HH}$ is the generalized aerodynamic force matrix, computed from the aerodynamic influence coefficient matrix, $\underline{\text{AIC}}$, as:

$$\underline{Q}_{HH} = \underline{\Phi}^T \cdot \underline{AIC} \cdot \underline{\Phi} \tag{43}$$

Matrix $\underline{Q}_{HH}$ is provided for harmonic motion as a function of reduced frequency, Mach number, and angle of attack (if a nonlinear unsteady aerodynamic model is used). In this study, the focus is on the inertial effect of maneuvering on flutter, all stability analyses were solved with $\underline{Q}_{HH}$ calculated at zero Mach number and angle of attack.

$\underline{\widetilde{\Omega}}^n$ was calculated for coordinated turn maneuvers of different load factors, $n$, and flight speed, $V$. In a coordinated turn, we can use the relations

$$\phi = \frac{1}{\arccos(n)} \qquad \dot{\psi} = \frac{g \tan(\phi)}{V} \tag{44}$$

from which

$$p = -\sin(\theta)\dot{\psi} \qquad q = \cos(\theta)\sin(\phi)\dot{\psi} \qquad r = \cos(\theta)\cos(\phi)\dot{\psi} \tag{45}$$

To simplify the analysis, $\theta$ was assumed to be zero. Also, the only coupling term considered is $\underline{G\Omega}$ to identify its distinctive effect.

Figure 6 and Table 3 show results of flutter analysis in a coordinated turn of $n = 5g$ compared with straight and level flight, $n = 1g$. It is evident that the critical mechanism S1 was destabilized, while mechanism S2 was stabilized, and A1 remained unchanged. For the S1 mechanism, the flutter onset speed was reduced as the load factor increased (by 2.6% at $n = 5g$) and the flutter frequency was slightly increased. The max modal damping was decreased by 4%.

| | **Mech S1** | | **Mech A1** | | **Mech S2** | | |
|---|---|---|---|---|---|---|---|
| **n load factor** | $f_f\ [Hz]$ | $V_f\ [\frac{m}{s}]$ | $f_f\ [Hz]$ | $V_f\ [\frac{m}{s}]$ | $f_f\ [Hz]$ | $V_f\ [\frac{m}{s}]$ | max g |
| 1 g | 4.22 | 24.2 | 6.57 | 26.3 | 7.55 | 29.3 | 2.2 % |
| 3 g | 4.26 (1.2%) | 23.9 (1.5%) | 6.58 (0%) | 26.3 (0%) | 7.44 (1.5%) | 29.8 (1.5%) | 1.6 % |
| 5 g | 4.31 (2.4%) | 23.6 (2.6%) | 6.58 (0%) | 26.3 (0%) | 7.34 (3%) | 30.3 (3%) | 1.1 % |

Table 3: A3TB flutter analysis characteristics in coordinated turn of different load factors

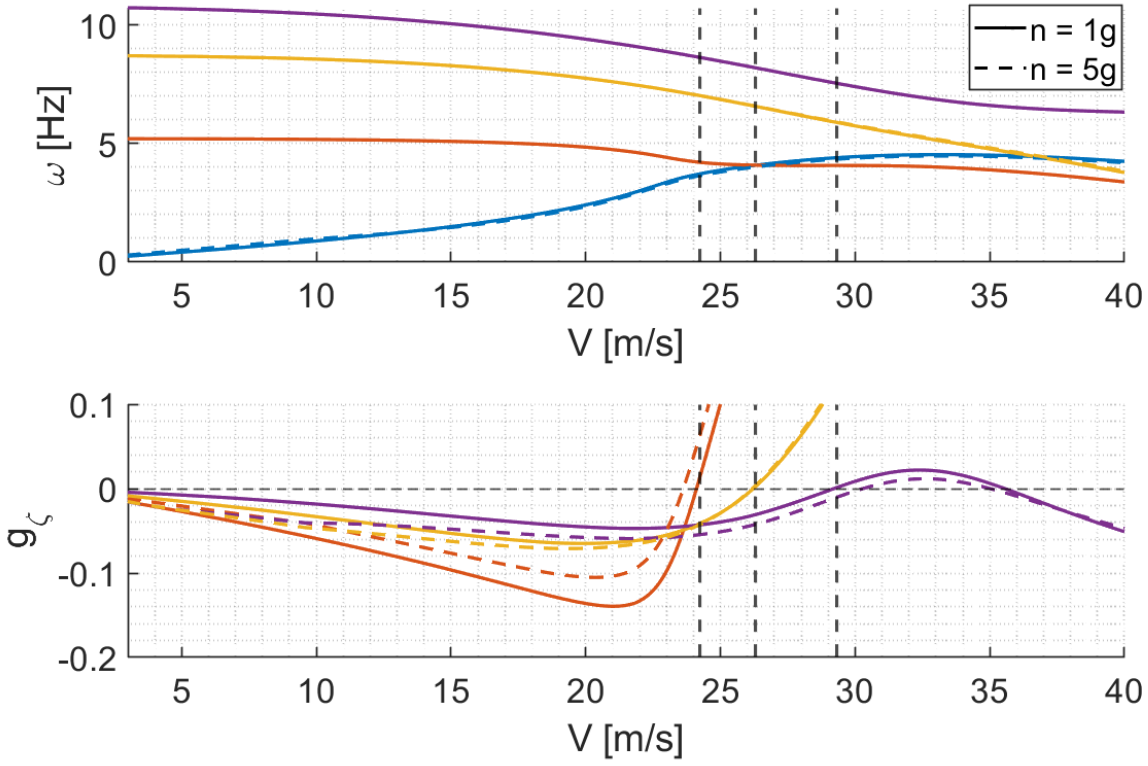


Figure 6: $\omega - V - g$ plot comparing the aeroelastic frequencies and damping values as a function of airspeed as computed at straight and level flight, $n = 1g$ and a coordinated turn of $n = 5g$

## 5 CONCLUSIONS

The paper presented an original derivation of the nonlinear coupled flight-mechanics - aeroelastic EOM of flexible and very flexible aircraft that were used to investigate the effect of inertial coupling during light and hard maneuvering. The set of nonlinear EOM involves both weak (non-acceleration related) and strong (acceleration related) coupling terms. It follows from the latter terms that under large deformations or during hard maneuvering, the rigid and elastic EOM must be solved concurrently. Each of the inertial coupling terms was examined to comprehend its magnitude and effect on the aircraft's rigid and elastic stability. The nonlinear EOM were linearized about a general nominal equilibrium state. A significant simplification of the EOM was achieved by introducing the modal coordinates of the coupled linearized EOM. The derivation introduced four new coupling terms: three damping terms and one stiffness term, where all coupling terms are functions of only the flight velocity and the load factor. The linearized EOM in modal coordinated were used in flutter analysis to compute flutter onset and characteristics during a coordinated turn of a user-defined load factor. Results of a $n = 5g$ coordinated turn were compared with those of straight and level flight, showing a reduced flutter onset speed of about 3% of the critical flutter mechanism of the examined test case configuration. Results of this study indicate that not accounting for maneuvering coupling effects in flutter analysis, as is typically done in production analyses, might lead to unconservative flutter predictions. Future work will further explore other configurations at different maneuvering conditions.

## REFERENCES

[1] Su, W. and Cesnik, C. E. (2014). Strain-based analysis for geometrically nonlinear beams: a modal approach. *Journal of Aircraft*, 51(3), 890–903.

[2] Cea, A. and Palacios, R. (2019). Nonlinear modal aeroelastic analysis from large industrial-scale models. In *AIAA Scitech 2019 Forum*. p. 208.

[3] Love, M., Zink, P., Wieselmann, P., et al. (2005). Body freedom flutter of high aspect ratio flying wings. In *46th AIAA/ASME/ASCE/AHS/ASC Structures, Structural Dynamics and Materials Conference*. p. 1947.

[4] Saltari, F., Riso, C., Matteis, G. D., et al. (2017). Finite-element-based modeling for flight dynamics and aeroelasticity of flexible aircraft. *Journal of Aircraft*, 54(6), 2350–2366.

[5] Baldelli, D. H., Chen, P. C., and Panza, J. (2006). Unified aeroelastic and flight dynamic formulation via rational function approximations. *Journal of Aircraft*, 43(3), 763–772.

[6] Joels, T., Yechieli, N., Edery-Azulay, L., et al. (2022). Design, analyses, and flutter testing of the Active Aeroelastic Aircraft Testbed (A3TB) platform. In *AIAA SCITECH 2022 Forum*. p. 2419.

[7] Milne, R. D. (1964). Dynamics of the deformable aeroplane. part 1. the equations of motion. part 2. a study of the trim state and longitudinal stability of the slender integrated aeroplane configuration. Tech. rep., Aeronautical Research Council, London, UK.

[8] Meirovitch, L. (1991). Hybrid state equations of motion for flexible bodies in terms of quasi-coordinates. *Journal of Guidance, Control, and Dynamics*, 14(5), 1008–1013.

[9] Nikravesh, P. E. (2005). Understanding mean-axis conditions as floating reference frames. *Advances in Computational Multibody Systems*, 185–203.

[10] Schmidt, D. K. and Raney, D. L. (2001). Modeling and simulation of flexible flight vehicles. *Journal of Guidance, Control, and Dynamics*, 24(3), 539–546.

[11] Chen, G., Sun, J., Mao, W., et al. (2016). Zaero theoretical manual. *ZONA Technology Inc*, 8.

[12] Palacios, R., Murua, J., and Cook, R. (2010). Structural and aerodynamic models in nonlinear flight dynamics of very flexible aircraft. *AIAA journal*, 48(11), 2648–2659.

[13] Rao, S. S. (2017). *The finite element method in engineering*. Butterworth-heinemann.

[14] Goizueta, N., Wynn, A., Palacios, R., et al. (2022). Flutter predictions for very flexible wing wind tunnel test. *Journal of Aircraft*, 59(4), 1082–1097.

[15] Beranek, J., Nicolai, L., Buonanno, M., et al. (2010). Conceptual design of a multi-utility aeroelastic demonstrator. In *13th AIAA/ISSMO Multidisciplinary Analysis Optimization Conference*.

[16] MacNeal, R. (1970). *NASTRAN theoretical manual*, vol. 221. Scientific and Technical Information Office, National Aeronautics and Space.

[17] Gu, Y. and Yang, Z. (2012). Modified pk method for flutter solution with damping iteration. *AIAA journal*, 50(2), 507–510.

[18] Eldred, M., Venkayya, V., and Anderson, W. (1995). New mode tracking methods in aeroelastic analysis. *AIAA journal*, 33(7), 1292–1299.

[19] Waszak, M. R. and Schmidt, D. K. (1988). Flight dynamics of aeroelastic vehicles. *Journal of Aircraft*, 25(6), 563–571.

# Appendices

## A THE CHOICE OF COORDINATE SYSTEM AND NONLINEAR EOM DERIVATION

The derivation of the coupled flight-dynamics and aeroelastic EOM is presented in the literature using several local coordinate systems, which are selected to either minimize the rigid-body and elastic coupling or to gain insight into the observed phenomena. In this appendix, we examine the different coordinate systems used in the literature, discuss their advantages and drawbacks, and justify the selection of the *Body Frame* in the current study coordinate system selection.

**Attached Axes.** Milne [7] proposed the Attached, Mean, and Principal Axes. The origin of the Attached frame is fixed to a point on the deformed body, and the axes' orientation is tangent to the curve of the deformed body at the local frame's origin (see figure 7(a)). The main advantage of the Attached Axes is that the origin can be placed anywhere on the body, such as at a sensor location. However, the origin's location and orientation vary with the elastic deformations, and thus the EOM expressed in those axes have coupling terms containing the CG location. In this coordinate system, the CG location (with respect to the local origin) is computed as:

$$\vec{r}_{cg} = \frac{1}{m}\underline{\widetilde{I}}^{T} \cdot \underline{M} \cdot \overline{r}_b \tag{A1}$$

**Mean Axes.** The *Mean Axes* were used in several studies [9, 10, 19] as they offer the benefit of inertial decoupling. The Mean Axes' origin location and orientation are defined such that the relative linear and angular momentum due to elastic deformation are zero at all times. Using eq. 19, this can be stated as:

$$\begin{aligned} \vec{P}_0 &= m\vec{V}_0 \\ \vec{H}_0 &= \underline{I}_M \cdot \vec{\omega} \end{aligned} \tag{A2}$$

Using the Mean Axes eliminates the strong coupling (coupling of the acceleration terms) of the elastic motion and the CG's translational and rotational motions. In this coordinate system, there is no connection between the aircraft's and the coordinate system's orientations since the coordinate system orientation is the same as if the aircraft was perfectly rigid (there are no external moments due to elastic motion). Determining the orientation of the Mean Axes with respect to the aircraft orientation is nontrivial; thus, in small deformation cases, equivalent conditions (termed "Practical Mean Axes") are derived to determine the Mean Axes' orientation [7]. In large deformations, the assumption of a small rotation from the orientation of the undeformed structure, used for the Practical Mean Axes equations derivation, is not valid; thus, the Practical Mean Axes cannot be used, and determining the Mean Axes' orientation by its definition is significantly more complex. This coordinate system is defined by the following constraints:

$$\underline{\widetilde{I}}^{T} \cdot \underline{M} \cdot \dot{\vec{u}}_e = 0 \qquad \& \qquad \underline{R}_b^T \cdot \underline{M} \cdot \dot{\vec{u}}_e = 0 \tag{A3}$$

The orientation of the Mean Axes is shown in figure 7(b).

**Body Axes.** The coordinate system used in the current study is the *Body Axes* [4]. The origin of the Body Axes is at the instantaneous CG location (which we refer to as the *floating CG*, since in an elastically deformed body, it may not reside on the body itself). The coordinate frame's orientation follows the rotating rigid body, and might change with the elastic motion.

This implies that an elastic motion does not create linear momentum but could create angular momentum, which is expressed as an external moment on the body. In Body Axes, the origin moves in the same transitional and rotational motion as the aircraft's CG, and thus, the EOM in Body Axes have fewer coupling terms than in Attached Axes. Furthermore, the Body Axes are frequently used in flight dynamics, offering a more intuitive understanding of flight dynamics effects. This coordinate system is defined by the following constraint:

$$\vec{r}_{cg} = \frac{1}{m}\underline{\widetilde{I}}^T \cdot \underline{M} \cdot \overline{r}_b = 0 \quad \rightarrow \quad \underline{\widetilde{I}}^T \cdot \underline{M} \cdot \overline{u}_e = 0 \tag{A4}$$

By time-derivation of the above in an inertial system and assuming a constant mass matrix we obtain:

$$\underline{\widetilde{I}}^T \cdot \underline{M} \cdot \dot{\overline{u}}_e = \underline{\widetilde{I}}^T \cdot \underline{M} \cdot \ddot{\overline{u}}_e = 0 \tag{A5}$$

Figure 7 shows the difference in the orientation of the Attached, Mean, and Body local frames, with respect to the rigid orientation of the aircraft (due to elastic motion only).

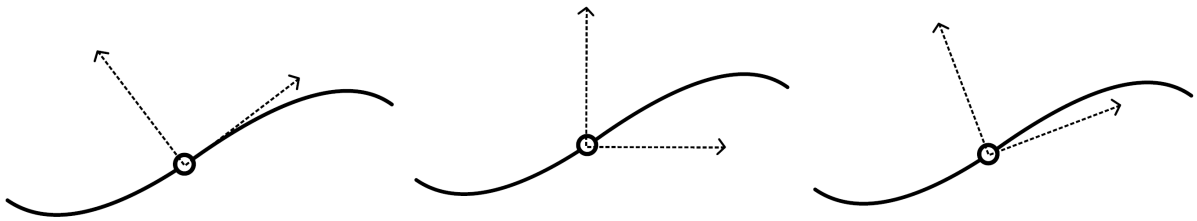

(a) Attached Axes (b) Mean Axes (c) Body Axes

Figure 7: The reference frames orientation due to anti-symmetric elastic motion (no external rigid moments)

**Principle Axes.** In the *Principle Axes*, the origin remains at the floating CG, and the orientation is defined such that the inertia matrix is diagonal. Thus, in Principal Axes, the CG's rotational EOM are decoupled. However, unlike in Body Axes, where the axes orientation changes due to elastic velocity and acceleration, the Principal Axes' orientation changes even due to elastic deformations, making the interpretation of the physical phenomena involved non-intuitive.

**Stability Axes.** Another practical coordinate system is the *Stability Axes* [5], which are defined similarly to the Body Axes but rotated such that the steady-state angle of attack and angle of slip are zero. Stability Axes have all the advantages of the Body Axes and are very useful for stability analysis and light maneuvering responses, in which the small perturbations assumption is valid. For hard maneuvering and large deformations, the angles of attack and slip cannot be assumed small, and thus the Stability Axes do not have an advantage over the Body Axes. Moreover, the Stability Axes are constant relative to the rigid body but must be pre-defined per configuration, weight, flight conditions, and maneuver.

### A.1 Derivation of the Nonlinear EOM

The time derivatives of the momenta of the deformed structure (eq. 19) with respect to the Inertial frame are:

$$\begin{aligned}
\frac{d\overline{p}_{bi}}{dt} =& \underline{M}\cdot\left(\widetilde{\underline{I}}\cdot\dot{\vec{V}}_0+\ddot{\overline{u}}_e-\underline{R}_b\cdot\dot{\vec{\omega}}+\widetilde{\underline{\Omega}}\cdot\dot{\overline{u}}_e\right)+\widetilde{\underline{\Omega}}\cdot\underline{M}\cdot\left(\widetilde{\underline{I}}\cdot\vec{V}_0+\dot{\overline{u}}_e+\widetilde{\underline{\Omega}}\cdot\overline{r}_b\right)\\
\frac{d\vec{P}_0}{dt} =& m\dot{\vec{V}}_0+\widetilde{\underline{I}}^T\cdot\underline{M}\cdot\ddot{\overline{u}}_e+\vec{\omega}\times\left(m\vec{V}_0+\widetilde{\underline{I}}^T\cdot\underline{M}\cdot\dot{\overline{u}}_e+m\vec{\omega}\times\vec{r}_{cg}\right)+m(\vec{\omega}\times\dot{\vec{r}}_{cg}+\dot{\vec{\omega}}\times\vec{r}_{cg})\\
\frac{d\vec{H}_0}{dt} =& \underline{I}_M\cdot\dot{\vec{\omega}}-\underline{R}_b^T\cdot\underline{M}\cdot\ddot{\overline{u}}_e+\vec{\omega}\times\left(\underline{I}_M\cdot\vec{\omega}-\underline{R}_b^T\cdot\underline{M}\cdot\dot{\overline{u}}_e+m\vec{r}_{cg}\times\vec{V}_0\right)\\
&+\dot{\underline{I}}_M\cdot\vec{\omega}-\dot{\underline{R}}_b^T\cdot\underline{M}\cdot\dot{\overline{u}}_e+m(\dot{\vec{r}}_{cg}\times\vec{V}_0+\vec{r}_{cg}\times\dot{\vec{V}}_0)
\end{aligned}\tag{A6}$$

Using Newton's second law

$$\begin{aligned}
\frac{d\overline{p}_{bi}}{dt} =& \overline{F}_{ex}+\underline{M}\cdot\widetilde{\underline{I}}\cdot\vec{g}-\underline{K}\cdot\overline{u}_e\\
\frac{d\vec{P}_0}{dt} =& \widetilde{\underline{I}}^T\cdot\overline{F}_{ex}+m\vec{g}\\
\frac{d\vec{H}_0}{dt} =& -\underline{R}_b^T\cdot\overline{F}_{ex}+m\vec{r}_{cg}\times\vec{g}
\end{aligned}\tag{A7}$$

where $\overline{F}_{ex}$ is the external load vector (due to aerodynamics, thrust, etc.) and $\vec{g}$ is the gravity acceleration vector.

Equating eq. A6 and A7[10], we get the coupled rigid-body and elastic EOM, summarized as follows:

$$\begin{bmatrix} m\underline{I} & -m\underline{R}_{cg} & \widetilde{\underline{I}}^T\cdot\underline{M}\\ m\underline{R}_{cg} & \underline{I}_M & -\underline{R}_b^T\cdot\underline{M}\\ \underline{M}\cdot\widetilde{\underline{I}} & -\underline{M}\cdot\underline{R}_b & \underline{M}\end{bmatrix}\cdot\begin{bmatrix}\dot{\vec{V}}_0\\ \dot{\vec{\omega}}\\ \ddot{\overline{u}}_e\end{bmatrix}=\begin{bmatrix}R\vec{H}S_L\\ R\vec{H}S_A\\ R\vec{H}S_E\end{bmatrix}\tag{A8}$$

where:

$$\begin{aligned}
R\vec{H}S_L =& -\vec{\omega}\times\left(m\vec{V}_0+2m\dot{\vec{r}}_{cg}+m\vec{\omega}\times\vec{r}_{cg}\right)+\widetilde{\underline{I}}^T\cdot\overline{F}_{ex}+m\vec{g}\\
R\vec{H}S_A =& -\vec{\omega}\times\left(\underline{I}_M\cdot\vec{\omega}-\underline{R}_b^T\cdot\underline{M}\cdot\dot{\overline{u}}_e+m\vec{r}_{cg}\times\vec{V}_0\right)-m\dot{\vec{r}}_{cg}\times\vec{V}_0\\
&-\dot{\underline{I}}_M\cdot\vec{\omega}+\dot{\underline{R}}_b^T\cdot\underline{M}\cdot\dot{\overline{u}}_e-\underline{R}_b^T\cdot\overline{F}_{ex}+m\vec{r}_{cg}\times\vec{g}\\
R\vec{H}S_E =& -\left(\underline{M}\cdot\widetilde{\underline{\Omega}}+\widetilde{\underline{\Omega}}\cdot\underline{M}\right)\cdot\dot{\overline{u}}_e-\widetilde{\underline{\Omega}}\cdot\underline{M}\cdot\widetilde{\underline{I}}\cdot\vec{V}_0-\widetilde{\underline{\Omega}}\cdot\underline{M}\cdot\widetilde{\underline{\Omega}}\cdot\overline{r}_b\\
&+\overline{F}_{ex}+\underline{M}\cdot\widetilde{\underline{I}}\cdot\vec{g}-\underline{K}\cdot\overline{u}_e
\end{aligned}\tag{A9}$$

$\underline{R}_{cg}\in\mathbb{R}^{3\times3}$ is the skew-symmetric representation of the physical vector $\vec{r}_{cg}$ (see eq. 5) that satisfies:

$$m\underline{R}_{cg}=\widetilde{\underline{I}}^T\cdot\underline{M}\cdot\underline{R}_b\tag{A10}$$

The green color represents rigid body terms, the blue color represents terms that are zero in Body and Mean Axes, and the red color represents terms that are zero only in Mean Axes.

[10]Note that due to the use of angular velocity in the derivation, the time derivative of linear momentum does not equal mass times body acceleration, and the latter cannot be utilized here.

## B EOM LINEARIZATION

Each kinematic parameter in the nonlinear EOM (eq. 21) can be divided into a nominal part, in the steady state, and a disturbance from that state as follows:

$$\vec{V}_0 = \vec{V}_0^n + \delta\vec{V}_0 \qquad \vec{\omega} = \vec{\omega}^n + \delta\vec{\omega} \qquad \overline{u}_e = \overline{u}_e^n + \delta\overline{u}_e \tag{B1}$$

Note that in the steady steady the following relations can be assumed:

$$\dot{\vec{V}}_0^n = 0 \qquad \dot{\vec{\omega}}^n = 0 \qquad \ddot{\overline{u}}_e^n = \dot{\overline{u}}_e^n = 0 \tag{B2}$$

The nominal state satisfies the nonlinear EOM, eq. 21, which are repeated here for clarity:

$$\begin{bmatrix} m\underline{I} & \underline{0} & \underline{0} \\ \underline{0} & \underline{I}_M & -\underline{R}_b^T \cdot \underline{M} \\ \underline{M} \cdot \widetilde{\underline{I}} & -\underline{M} \cdot \underline{R}_b & \underline{M} \end{bmatrix} \cdot \begin{bmatrix} \dot{\vec{V}}_0 \\ \dot{\vec{\omega}} \\ \ddot{\overline{u}}_e \end{bmatrix} = \begin{bmatrix} \overrightarrow{RHS}_T \\ \overrightarrow{RHS}_R \\ \overrightarrow{RHS}_E \end{bmatrix} \tag{B3}$$

where:

$$\begin{aligned} \overrightarrow{RHS}_T &= -m\vec{\omega} \times \vec{V}_0 + \widetilde{\underline{I}}^T \cdot \overline{F}_{ex} + m\vec{g} \\ \overrightarrow{RHS}_R &= -\vec{\omega} \times \left(\underline{I}_M \cdot \vec{\omega} - \underline{R}_b^T \cdot \underline{M} \cdot \dot{\overline{u}}_e\right) - \dot{\underline{I}}_M \cdot \vec{\omega} + \dot{\underline{R}}_b^T \cdot \underline{M} \cdot \dot{\overline{u}}_e - \underline{R}_b^T \cdot \overline{F}_{ex} \\ \overrightarrow{RHS}_E &= -\left(\underline{M} \cdot \widetilde{\underline{\Omega}} + \widetilde{\underline{\Omega}} \cdot \underline{M}\right) \cdot \dot{\overline{u}}_e - \widetilde{\underline{\Omega}} \cdot \underline{M} \cdot \widetilde{\underline{I}} \cdot \vec{V}_0 - \widetilde{\underline{\Omega}} \cdot \underline{M} \cdot \widetilde{\underline{\Omega}} \cdot \overline{r}_b \\ &\quad + \overline{F}_{ex} + \underline{M} \cdot \widetilde{\underline{I}} \cdot \vec{g} - \underline{K} \cdot \overline{u}_e \end{aligned} \tag{B4}$$

Assigning the relations of eq. B2 into eq. B3 yields:

$$\begin{aligned} m\vec{\omega}^n \times \vec{V}_0^n - \widetilde{\underline{I}}^T \cdot \overline{F}_{ex}^n - m\vec{g} = 0 \\ \vec{\omega}^n \times \underline{I}_M^n \cdot \vec{\omega}^n + \underline{R}_b^{nT} \cdot \overline{F}_{ex}^n = 0 \\ \widetilde{\underline{\Omega}}^n \cdot \underline{M} \cdot \widetilde{\underline{I}} \cdot \vec{V}_0^n + \widetilde{\underline{\Omega}}^n \cdot \underline{M} \cdot \widetilde{\underline{\Omega}} \cdot \overline{r}_b^n - \overline{F}_{ex}^n - \underline{M} \cdot \widetilde{\underline{I}} \cdot \vec{g} + \underline{K} \cdot \overline{u}_e^n = 0 \end{aligned} \tag{B5}$$

Eqs. B1, B2, B5 are used to linearize eq.B3 (neglecting any high order disturbance terms), yielding:

$$\begin{aligned} &m\delta\dot{\vec{V}}_0 = -m\vec{\omega}^n \times \delta\vec{V}_0 - m\delta\vec{\omega} \times \vec{V}_0^n + \widetilde{\underline{I}}^T \cdot \delta\overline{F}_{ex} \\ &\underline{I}_M^n \cdot \delta\dot{\vec{\omega}} - \underline{R}_b^{nT} \cdot \underline{M} \cdot \delta\ddot{\overline{u}}_e = -\delta\vec{\omega} \times (\underline{I}_M^n \cdot \vec{\omega}^n) - \vec{\omega}^n \times (\delta\underline{I}_M \cdot \vec{\omega}^n) - \vec{\omega}^n \times (\underline{I}_M^n \cdot \delta\vec{\omega}) \\ &\qquad + \vec{\omega}^n \times (\underline{R}_b^{nT} \cdot \underline{M} \cdot \delta\dot{\overline{u}}_e) - \delta\dot{\underline{I}}_M \cdot \vec{\omega}^n - \delta\underline{R}_b^T \cdot \overline{F}_{ex}^n - \underline{R}_b^{nT} \cdot \delta\overline{F}_{ex} \\ &\underline{M} \cdot \widetilde{\underline{I}} \cdot \delta\dot{\vec{V}}_0 - \underline{M} \cdot \underline{R}_b^n \cdot \delta\dot{\vec{\omega}} + \underline{M} \cdot \delta\ddot{\overline{u}}_e = \\ &\qquad - \underline{M} \cdot \widetilde{\underline{\Omega}}^n \cdot \delta\dot{\overline{u}}_e + \widetilde{\underline{\Omega}}^n \cdot \underline{M} \cdot \delta\dot{\overline{u}}_e - \delta\widetilde{\underline{\Omega}} \cdot \underline{M} \cdot \widetilde{\underline{I}} \cdot \vec{V}_0^n - \widetilde{\underline{\Omega}}^n \cdot \underline{M} \cdot \widetilde{\underline{I}} \cdot \delta\vec{V}_0 \\ &\qquad - \delta\widetilde{\underline{\Omega}} \cdot \underline{M} \cdot \widetilde{\underline{\Omega}}^n \cdot \overline{r}_b^n - \widetilde{\underline{\Omega}}^n \cdot \underline{M} \cdot \delta\widetilde{\underline{\Omega}} \cdot \overline{r}_b^n - \widetilde{\underline{\Omega}}^n \cdot \underline{M} \cdot \widetilde{\underline{\Omega}}^n \cdot \delta\overline{r}_b + \delta\overline{F}_{ex} - \underline{K} \cdot \delta\overline{u}_e \end{aligned} \tag{B6}$$

where:

$$\delta\underline{I}_M = 2\underline{R}_b^{nT} \cdot \underline{M} \cdot \delta\underline{R}_b \qquad \delta\overline{r}_b = \delta\overline{r}_{b0} + \delta\overline{u}_e \tag{B7}$$

where $\delta\widetilde{\underline{\Omega}}$ is the block-diagonal extension of the skew-symmetric representation of $\delta\vec{\omega}$ (see eq. 14) and $\delta\underline{R}_b$ is the skew-symmetric representation of $\delta\overline{r}_b$.

### B.1 Linearized EOM in Modal Coordinates

Using the modal representation in eq 34, the rigid and elastic displacements and their time derivatives in the Inertial frame can be written as:

$$\begin{aligned}
\underline{\Phi}_e \cdot \overline{\xi}_e &= \delta\overline{u}_e & \underline{\Phi}_r \cdot \overline{\xi}_r &= \widetilde{\underline{I}} \cdot \delta\vec{r}_0 + \delta\overline{r}_{b0} \\
\underline{\Phi}_e \cdot \dot{\overline{\xi}}_e &= \delta\dot{\overline{u}}_e + \widetilde{\underline{\Omega}}^n \cdot \delta\overline{u}_e & \underline{\Phi}_r \cdot \dot{\overline{\xi}}_r &= \widetilde{\underline{I}} \cdot \delta\vec{V}_0 + \delta\widetilde{\underline{\Omega}} \cdot \overline{r}^n_{b0} \\
\underline{\Phi}_e \cdot \ddot{\overline{\xi}}_e &= \delta\ddot{\overline{u}}_e + \dot{\widetilde{\underline{\Omega}}}^n \cdot \delta\overline{u}_e + 2\widetilde{\underline{\Omega}}^n \cdot \delta\dot{\overline{u}}_e + \widetilde{\underline{\Omega}}^n \cdot \widetilde{\underline{\Omega}} \cdot \delta\overline{u}_e & \underline{\Phi}_r \cdot \ddot{\overline{\xi}}_r &= \widetilde{\underline{I}} \cdot \delta\dot{\vec{V}}_0 + \delta\dot{\widetilde{\underline{\Omega}}} \cdot \overline{r}^n_{b0} + \widetilde{\underline{\Omega}}^n \cdot (\widetilde{\underline{I}} \cdot \delta\vec{V}_0 + \delta\widetilde{\underline{\Omega}} \cdot \overline{r}_{b0})
\end{aligned} \tag{B8}$$

Note that here, the time derivatives $\underline{\Phi}_r \cdot \dot{\overline{\xi}}_r$, $\underline{\Phi}_e \cdot \dot{\overline{\xi}}_e$, $\underline{\Phi}_r \cdot \ddot{\overline{\xi}}_r$, and $\underline{\Phi}_e \cdot \ddot{\overline{\xi}}_e$ are *inertial derivatives*.[11] From eq. B8, we can derive the expression for the elastic deformations and their relative time derivatives and other useful relations.

$$\begin{aligned}
\delta\overline{u}_e &= \underline{\Phi}_e \cdot \overline{\xi}_e & \widetilde{\underline{I}} \cdot \delta\vec{r}_0 + \delta\overline{r}_{b0} &= \underline{\Phi}_r \cdot \overline{\xi}_r \\
\delta\dot{\overline{u}}_e &= \underline{\Phi}_e \cdot \dot{\overline{\xi}}_e - \widetilde{\underline{\Omega}}^n \cdot \underline{\Phi}_e \cdot \overline{\xi}_e & \widetilde{\underline{I}} \cdot \delta\vec{V}_0 - \underline{R}^n_b \cdot \delta\vec{\omega} &= \underline{\Phi}_r \cdot \dot{\overline{\xi}}_r + \delta\widetilde{\underline{\Omega}} \cdot \overline{u}^n_e \\
\delta\ddot{\overline{u}}_e &= \underline{\Phi}_e \cdot \ddot{\overline{\xi}}_e - \dot{\widetilde{\underline{\Omega}}}^n \cdot \underline{\Phi}_e \cdot \overline{\xi}_e - 2\widetilde{\underline{\Omega}}^n \cdot \underline{\Phi}_e \cdot \dot{\overline{\xi}}_e + \widetilde{\underline{\Omega}}^n \cdot \widetilde{\underline{\Omega}}^n \cdot \underline{\Phi}_e \cdot \overline{\xi}_e & \widetilde{\underline{I}} \cdot \delta\dot{\vec{V}}_0 - \underline{R}^n_b \cdot \delta\dot{\vec{\omega}} &= \underline{\Phi}_r \cdot \ddot{\overline{\xi}}_r - \widetilde{\underline{\Omega}}^n \cdot \underline{\Phi}_r \cdot \dot{\overline{\xi}}_r + \delta\dot{\widetilde{\underline{\Omega}}} \cdot \overline{u}^n_e
\end{aligned} \tag{B9}$$

Using eqs. 32 and 34 we get (same as in eq. 16) :

$$\delta\overline{r}_{b0} = -\underline{R}^n_{b0} \cdot \underline{D}_R \cdot \underline{\Phi}_r \cdot \overline{\xi}_r \tag{B10}$$

where $\underline{R}^n_{b0} \in \mathbb{R}^{3N\times 3}$ is the skew-symmetric representation of $\overline{r}^n_{b0}$ (similar definition to $\underline{R}_b$, as in eq.8). For small angular disturbances, and by repeating the process as in eq. B10, we get:

$$\delta\vec{\omega} = \frac{d}{dt}\delta\vec{\vartheta} = \underline{D}_R \cdot \underline{\Phi}_r \cdot \dot{\overline{\xi}}_r \tag{B11}$$

From eqs. B6 & B9 we get the EOM in modal coordinates:

$$\begin{aligned}
&\underline{M} \cdot \underline{\Phi}_r \cdot \ddot{\overline{\xi}}_r + \underline{M} \cdot \underline{\Phi}_e \cdot \ddot{\overline{\xi}}_e + \left(\widetilde{\underline{\Omega}}^n \cdot \underline{M} - \underline{M} \cdot \widetilde{\underline{\Omega}}^n\right) \cdot \underline{\Phi}_r \cdot \dot{\overline{\xi}}_r + \left(\widetilde{\underline{\Omega}}^n \cdot \underline{M} - \underline{M} \cdot \widetilde{\underline{\Omega}}^n\right) \cdot \underline{\Phi}_e \cdot \dot{\overline{\xi}}_e \\
&+ \delta\widetilde{\underline{\Omega}} \cdot \underline{M} \cdot \left(\widetilde{\underline{I}} \cdot \vec{V}^n_0 + \widetilde{\underline{\Omega}}^n \cdot \overline{r}^n_b\right) + \widetilde{\underline{\Omega}}^n \cdot \underline{M} \cdot \delta\widetilde{\underline{\Omega}} \cdot \overline{u}^n_e + \widetilde{\underline{\Omega}}^n \cdot \underline{M} \cdot \widetilde{\underline{\Omega}}^n \cdot \delta\overline{r}_{b0} + \underline{K} \cdot \underline{\Phi}_e \cdot \overline{\xi}_e = \overline{F}_{ex}
\end{aligned} \tag{B12}$$

[11] This is different from the general notation used in this study, where $\frac{d()}{dt}$ is used for time derivative with respect to the Inertial frame, and $\dot{()}$ for time derivative with respect to the Body frame. Here, the notation was changed to align with the notation commonly used in aeroelasticity texts.